

## Article

# Design, Synthesis and Cytotoxic Activity Evaluation of Newly Synthesized Amides-Based TMP Moiety as Potential Anticancer Agents over HepG2 Cells

Tarfah Al-Warhi <sup>1</sup>, Adil Aldhahrani <sup>2</sup>, Fayez Althobaiti <sup>3</sup>, Eman Fayad <sup>3</sup> , Ola A. Abu Ali <sup>4</sup>, Sarah Albogami <sup>3</sup> , Ali H. Abu Almaaty <sup>5</sup> , Amgad I. M. Khedr <sup>6</sup>, Syed Nasir Abbas Bukhari <sup>7</sup>  and Islam Zaki <sup>8,\*</sup> 

- <sup>1</sup> Department of Chemistry, College of Science, Princess Nourah Bint Abdulrahman University, P.O. Box 84428, Riyadh 11671, Saudi Arabia; tarfah-w@hotmail.com
  - <sup>2</sup> Clinical Laboratory Sciences Department, Turabah University Faculty, Taif University, Taif 21995, Saudi Arabia; a.ahdhahrani@tu.edu.sa
  - <sup>3</sup> Department of Biotechnology, Faculty of Sciences, Taif University, P.O. Box 11099, Taif 21944, Saudi Arabia; faiz@tu.edu.sa (F.A.); e.email@tu.edu.sa (E.F.); dr.sarah@tu.edu.sa (S.A.)
  - <sup>4</sup> Department of Chemistry, College of Science, Taif University, P.O. Box 11099 Taif 21944, Saudi Arabia; o.abuali@tu.edu.sa
  - <sup>5</sup> Zoology Department, Faculty of Science, Port Said University, Port Said 42526, Egypt; ali\_zoology\_2010@yahoo.com
  - <sup>6</sup> Department of Pharmacognosy, Faculty of Pharmacy, Port Said University, Port Said 42526, Egypt; a\_mansour7799@yahoo.com
  - <sup>7</sup> Department of Pharmaceutical Chemistry, College of Pharmacy, Jouf University, Sakaka 72388, Saudi Arabia; sbukhari@ju.edu.sa
  - <sup>8</sup> Pharmaceutical Organic Chemistry Department, Faculty of Pharmacy, Port Said University, Port Said 42526, Egypt
- \* Correspondence: eslam.zaki@pharm.psu.edu.eg; Tel.: +20-1153436140



**Citation:** Al-Warhi, T.; Aldhahrani, A.; Althobaiti, F.; Fayad, E.; Abu Ali, O.A.; Albogami, S.; Abu Almaaty, A.H.; Khedr, A.I.M.; Bukhari, S.N.A.; Zaki, I. Design, Synthesis and Cytotoxic Activity Evaluation of Newly Synthesized Amides-Based TMP Moiety as Potential Anticancer Agents over HepG2 Cells. *Molecules* **2022**, *27*, 3960. <https://doi.org/10.3390/molecules27123960>

Academic Editors: Simona Collina and Arun Sharma

Received: 1 May 2022

Accepted: 7 June 2022

Published: 20 June 2022

**Publisher's Note:** MDPI stays neutral with regard to jurisdictional claims in published maps and institutional affiliations.



**Copyright:** © 2022 by the authors. Licensee MDPI, Basel, Switzerland. This article is an open access article distributed under the terms and conditions of the Creative Commons Attribution (CC BY) license (<https://creativecommons.org/licenses/by/4.0/>).

**Abstract:** A novel series of amides based TMP moiety was designed, synthesized and evaluated for their antiproliferative as well as enzyme inhibition activity. Compounds **6a** and **6b** showed remarkable cytotoxic activity against HepG2 cells with IC<sub>50</sub> values 0.65 and 0.92 μM, respectively compared with SAHA and CA-4 as reference compounds. In addition, compound **6a** demonstrated good HDAC-tubulin dual inhibition activity as it showed better HDAC activity as well as anti-tubulin activity. Moreover, compound **6a** exhibited G2/M phase arrest and pre-G1 apoptosis as demonstrated by cell cycle analysis and Annexin V assays. Further apoptosis studies demonstrated that compound **6a** boosted the level of caspase 3/7. Caspase 3/7 activation and apoptosis induction were evidenced by decrease in mitochondrial permeability suggesting that activation of caspase 3/7 may occur via mitochondrial apoptotic pathway.

**Keywords:** diamide; triamide; tetraamide; TMP; HDAC; tubulin; Annexin V; caspase; MMP

## 1. Introduction

Targeted-based anticancer therapy is one of the most important tactics for optimizing antitumor agents to avoid several drawbacks associated with traditional chemotherapeutic agents such as systemic toxicity, adverse side effects, absence of selective target and emergence of drug resistance [1–4]. Recently, researchers have focused on designing dual or multi-target anticancer agents which hold great advantages such as reverse drug resistance, improve therapeutic efficacy and seems to be an ideal solution to control cancer [5–7].

Histone deacetylases (HDACs) are epigenetic enzymes that have been regarded validated targets in inhibition of cancer cell proliferation and apoptosis induction [8,9]. HDACs enzymes catalyze the deacetylation from lysine residue in histone tails [10]. In addition, HDACs regulate signaling pathways via deacetylating large number of other nonhistones involved in gene expression [11]. High expression of aberrant recruitment of these enzymes

has been shown in a broad range of diseases including several types of cancer, cardiovascular and neurological diseases [12–14]. Therefore, HDACs inhibition is considered as highly attractive therapeutic targets for numerous disorders especially, malignancies and generating the interest toward vast number of HDACs inhibitors in various clinical trials [15,16].

HDAC inhibitors employing zinc chelating functionalities such as hydroxamates, benzamides, short chain fatty acids and ketones have shown promising results in cancer treatment [17]. Chidamide (I) is a benzamide HDAC inhibitor approved by the China food and drug administration for the treatment of refractory PTCL [18]. The 2-amino benzamide molecule MS-275 (II) represents another HDAC inhibitor in phase I/II clinical trials for the treatment of solid tumors [19]. In addition, compound III containing bulky group exhibited 10-fold and 20-fold potencies for HDAC1 compared with HDAC2 and HDAC3, respectively [20]. Moreover, compound IV displayed comparable pan HDAC inhibitory activity compared with IC<sub>50</sub> 4.648 μM, as compared with BG45 (IC<sub>50</sub> = 5.506 μM) [21] (Figure 1).

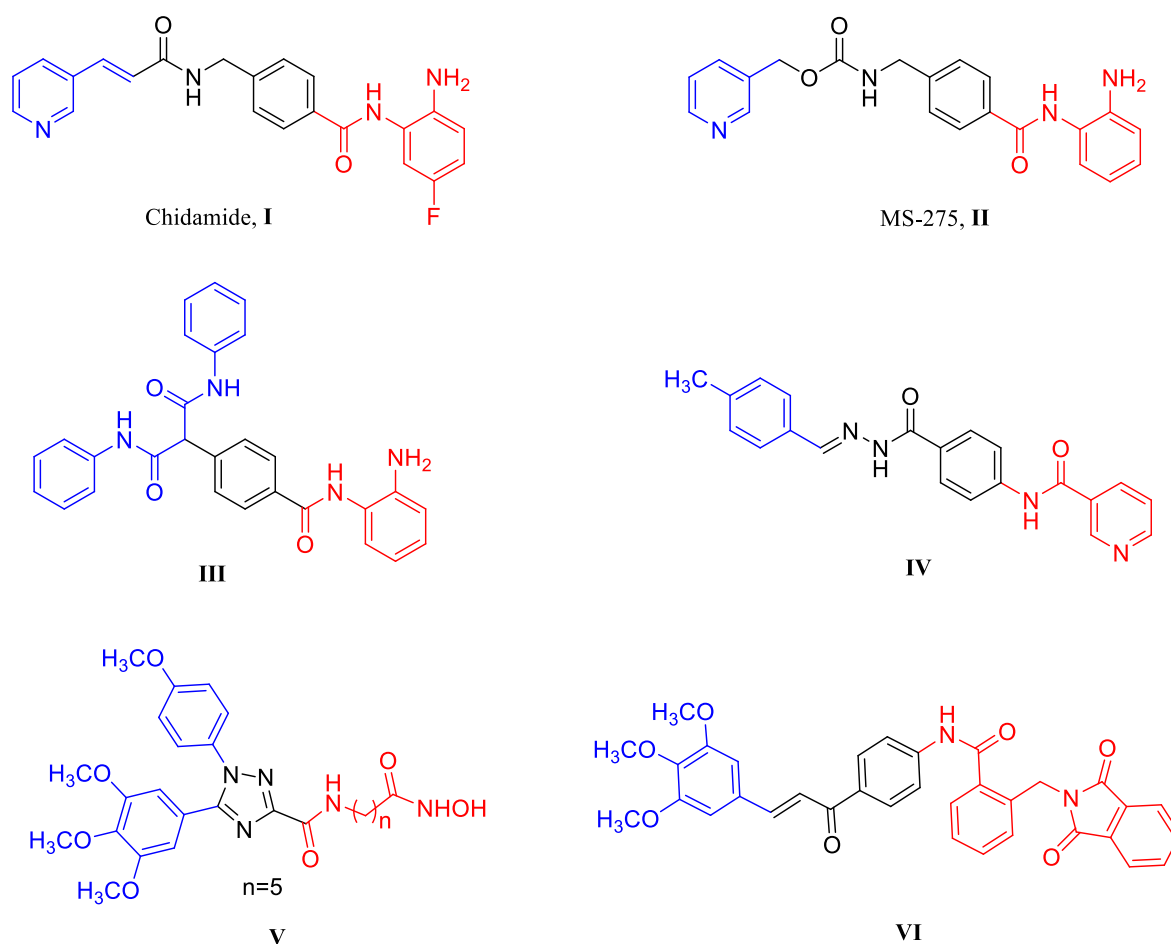


**Figure 1.** The structures of HDAC inhibitors in clinical trials (I–IV) and dual HDAC-tubulin inhibitors (V and VI). Cap group showed in blue color and zinc binding group showed in red color.

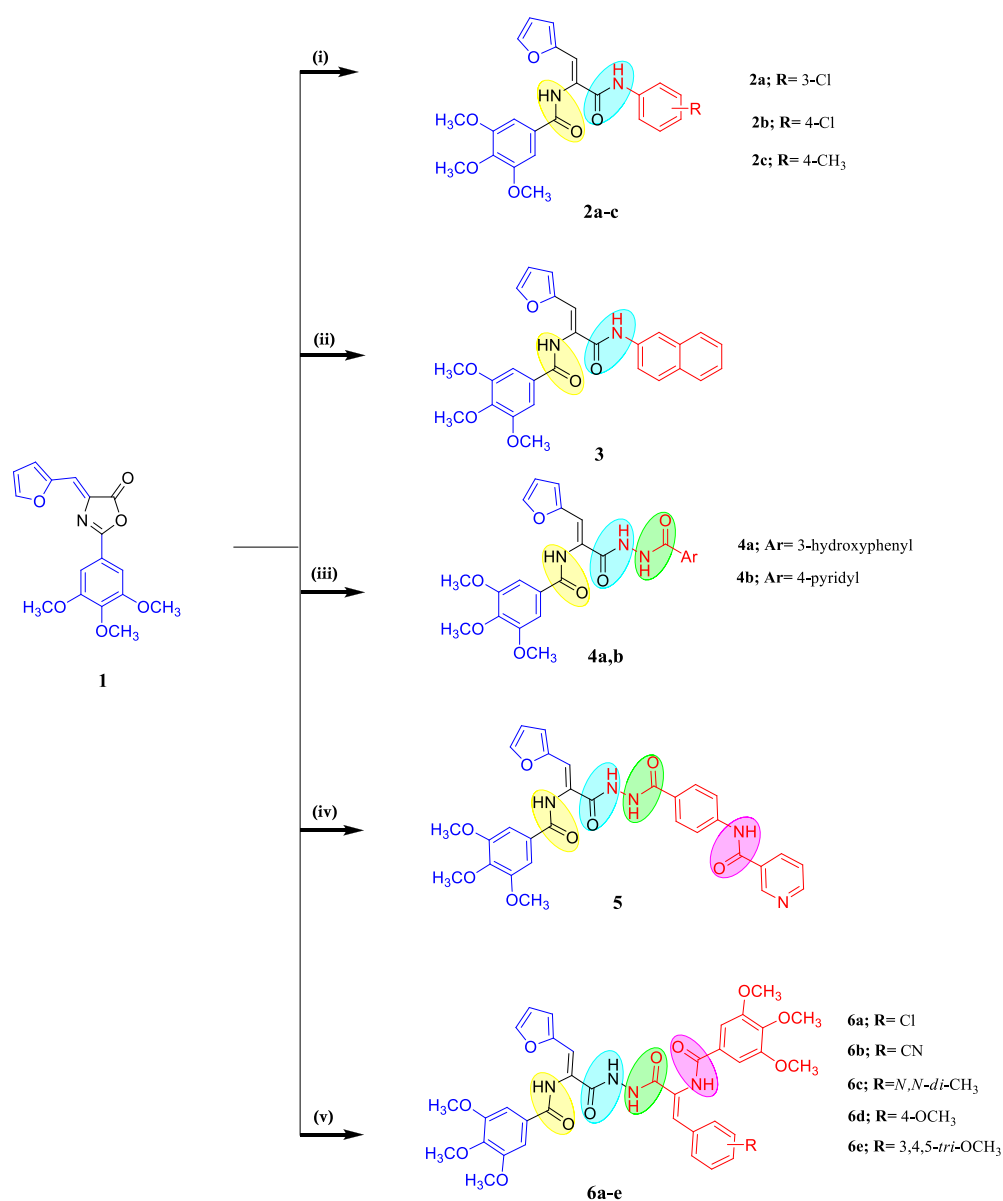
Several reported experimental studies proved that 3,4,5-trimethoxyphenyl (TMP) moiety is a privileged ring in several anticancer molecules such Colchicine (Col), combretastatin A-4 (CA-4) and their analogues [22–24]. The TMP ring exhibited promising anticancer activity mainly via inhibition of tubulin assembly into microtubules [25]. Interestingly, synergistic effect of HDACs inhibition and tubulin inhibition has been observed in many studies. For example, compound V and VI possessing TMP moiety and were demonstrated as potential HDAC-tubulin inhibitor [26,27].

Inspired by the above mentioned aspects and in continue efforts to discover new anticancer agents with better apoptotic properties [28,29], the present study concerned with the design and synthesis of novel series of amide-based compounds in the hopes of obtaining novel dual HDAC and tubulin inhibitors with promising anticancer potency. All the prepared amide compounds were screened for cytotoxicity against hepatocellular carcinoma HepG2 and normal liver cell line HL-7702 cell lines utilizing MTT antiproliferative assay. Moreover, apoptosis assays and cell cycle analysis of the most active molecule was carried out to detect if the cytotoxic potency is accompanied by change in cell cycle analysis and apoptosis induction. Furthermore, its ability to boost caspase 3/7 and decrease the MMP was investigated to show the apoptotic pathway mechanism.

## 2. Results and Discussion

### 2.1. Chemistry

The general approach leading to the synthesis of the target amide derivatives is outlined in Scheme 1. Ring opening of oxazolone **1** with respective aryl amine; namely 3-chloro aniline, 4-chloro aniline, 4-methyl aniline or 2-naphthyl amine in glacial acetic acid for 1–3 h provided the corresponding diamide compounds **2a–c** or **3**, respectively [30]. Structures of compounds **2a–c** and **3** were elucidated from their  $^1\text{H-NMR}$  and  $^{13}\text{C-NMR}$  spectral studies. The  $^1\text{H-NMR}$  spectra, the presence of two NH groups of the two amide functions was supported by two signals at  $\delta$  9.91–9.97 and 9.97–10.24 ppm, in addition to the presence of new signals at aromatic region at  $\delta$  6.62–8.14 ppm ascribed to new phenyl or naphthyl ring protons. In addition,  $^{13}\text{C-NMR}$  spectra of compounds **2a–c** and **3** revealed the presence of two peaks at  $\delta$  163.79–166.01 ppm corresponds to carbonyl (C=O) groups of the two amide functions. The desired triamide derivatives **4a,b** were obtained through oxazolone **1** reaction with respective aryl carbohydrazide in boiling pure ethanol.  $^1\text{H-NMR}$  spectra of the product **4b** as representative example exhibited signals of the three NH protons of the triamide function at  $\delta$  9.90, 10.32 and 10.80 ppm as well as the presence of extra proton signals in the region at  $\delta$  6.63–8.78 ppm related pyridyl function. In addition, signals of the carbonyl (C=O) groups of the triamide function were recorded in  $^{13}\text{C-NMR}$  spectra of compound **4b** at  $\delta$  164.48, 164.52 and 165.81 ppm. The target tetraamide derivative **5** was achieved by refluxing oxazolone **1** with *N*-[4-(hydrazine carbonyl)phenyl]nicotinamide in DMF containing catalytic amount of glacial acetic acid. In confirmation,  $^1\text{H-NMR}$  spectrum of compound **5** exhibited four signals at  $\delta$  9.87, 10.18, 10.40 and 10.68 ppm attributed to NH protons of four amide functions, in addition to new signals between  $\delta$  6.62–9.13 ppm integrating thirteen aromatic protons, and olefinic (=CH) proton. In the  $^{13}\text{C-NMR}$  spectrum, compound **5** exhibited four carbon signals at  $\delta$  164.61, 164.90, 165.45 and 165.75 ppm ascribed to carbonyl (C=O) groups of tetraamide function as well as the presence of extra signals related to phenyl and pyridyl carbons. In order to obtain the target tetraamide derivatives **6a–e**, various acrylic acid hydrazide molecules were used to synthesize the target compounds. The structure confirmations of tetraamide molecules **6a–e** were based on spectral studies such as  $^1\text{H-NMR}$  and  $^{13}\text{C-NMR}$  spectra.  $^1\text{H-NMR}$  spectra of **6a–e** exhibited four new signals in the region between  $\delta$  9.75–10.36 ppm ascribed to the four amide protons in addition to extra proton signals in the aromatic region corresponds to phenyl groups.  $^{13}\text{C-NMR}$  spectra of tetraamide **6a–e** confirmed the carbon skeleton due to the presence of four carbon signals at  $\delta$  163.98–165.77 ppm attributed to the carbonyl (C=O) functions of the four amide groups.



**Scheme 1.** Synthesis of the target compounds **2–6e**. Reagent and reaction condition: (i) respective aryl amine, AcOH, reflux 1–2 h; (ii) 2-naphthyl amine, AcOH, reflux 3 h; (iii) respective aryl carbohydrazide, ethanol, reflux 4–5 h; (iv) *N*-[4-(hydrazinecarbonyl)phenyl]nicotinamide, DMF, AcOH, reflux 6 h; (v) respective acrylic acid hydrazide, DMF, AcOH, reflux 6–8 h.

## 2.2. Biology

### 2.2.1. In Vitro Cytotoxic Activity against HepG2 Cell Line

The synthesized amide based compounds were subjected to MTT cell proliferation assay using suberoylanilide hydroxamic acid (SAHA) and CA-4 as positive reference compounds in this investigation. Results were reported as IC<sub>50</sub> values (μM) as shown in Table 1. Compounds **6a**, **6b** and **6c** were the most potent in this investigation with IC<sub>50</sub> values 0.65, 0.92 and 1.12 μM, respectively. Compound **6a** (IC<sub>50</sub> = 0.65 μM) was four folds more active than the SAHA (IC<sub>50</sub> = 2.91 μM) and nearly equipotent to reference compound CA-4 (IC<sub>50</sub> = 0.54 μM). Structurally, in the diamide series **2a–c** and **3**, naphthalene favors the anticancer activity rather substituted phenyl ring. This is obvious upon compound **3** (IC<sub>50</sub> = 16.24 μM) and compounds **2a–c** (IC<sub>50</sub> = 22.03–68.90 μM). In the triamide series **4a,b** compound **4b** bearing pyridyl function favors the anticancer activity (IC<sub>50</sub> = 8.36 μM) than 3-hydroxyphenyl moiety (IC<sub>50</sub> = 13.37 μM). Regarding the tetraamide series **5** and **6a–e**, compound **6a** was the most effective in cell proliferation in HepG2 cells with IC<sub>50</sub>

value 0.65  $\mu\text{M}$ . Moreover, compound **6a** proved to be selective toward normal liver cell line HL-7022 with selectivity ratio of 14.8.

**Table 1.** Cytotoxic screening of the tested amides 2a–6e. Values are the mean of three independent replicates  $\pm$  SE.

Comp No	IC <sub>50</sub> Value ( $\mu\text{M}$ )	
	HepG2	HL-7702
<b>2a</b>	68.90 $\pm$ 3.32	NT
<b>2b</b>	23.28 $\pm$ 1.03	NT
<b>2c</b>	22.03 $\pm$ 0.96	NT
<b>3</b>	16.24 $\pm$ 0.79	NT
<b>4a</b>	13.37 $\pm$ 0.56	NT
<b>4b</b>	8.36 $\pm$ 0.51	NT
<b>5</b>	3.25 $\pm$ 0.25	NT
<b>6a</b>	0.65 $\pm$ 0.03	9.62 $\pm$ 0.23
<b>6b</b>	0.92 $\pm$ 0.10	11.09 $\pm$ 0.18
<b>6c</b>	1.12 $\pm$ 0.12	9.88 $\pm$ 0.14
<b>6d</b>	3.81 $\pm$ 0.18	NT
<b>6e</b>	3.98 $\pm$ 0.09	NT
SAHA	2.91 $\pm$ 0.15	NT
CA-4	0.54 $\pm$ 0.04	8.86 $\pm$ 0.67

### 2.2.2. HDAC Inhibitory Activity

In order to cast light onto the mechanism of action of the prepared tetraamide based molecules, the most potent compound in the present study was investigated for its in vitro HDAC1 and HDAC2 inhibitory activity using human colorimetric simple ELISA kits and SAHA was taken as reference compound. Results in Figure 2 revealed that the tested tetraamide molecule **6a** showed significant inhibitory activity against HDAC1 and HDAC2 isoforms. It could be noticed that compound **6a** strongly inhibited HDAC1 and HDAC2 isoforms with IC<sub>50</sub> values 0.047 and 0.086  $\mu\text{M}$ , respectively compared with values of 0.028 and 0.072  $\mu\text{M}$  for SAHA, respectively.

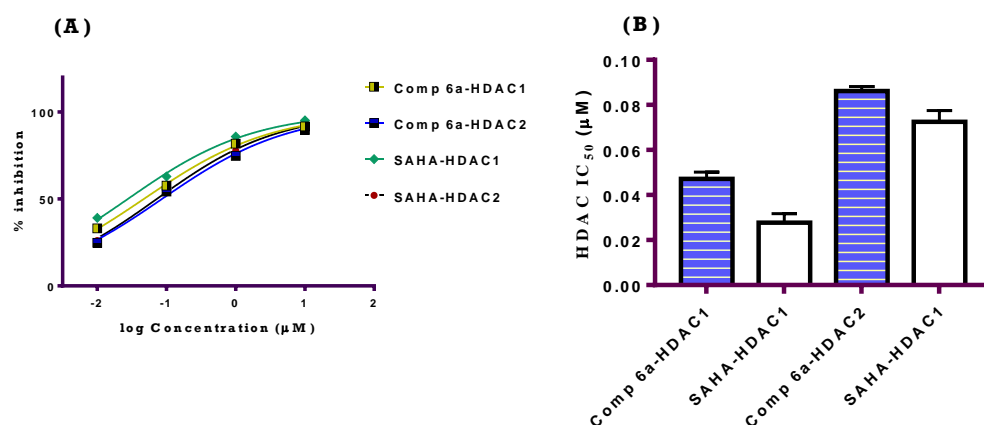


**Figure 2.** (A) Dose response curve for in vitro HDAC inhibitory activity of tetraamide **6a** and SAHA against HDAC1 and HDAC2 isoforms. (B) Graphical representation for in vitro HDAC inhibitory activity of tetraamide **6a** and SAHA against HDAC1 and HDAC2 isoforms.

### 2.2.3. Tubulin Polymerization Inhibition Assay

To evaluate the effect of the prepared amide derivatives on tubulin assembly in vitro, compound **6a** was evaluated for its tubulin polymerization inhibition activity using ELISA analysis. The results in Figure 3A revealed that the tetraamide derivative **6a** inhibited assembly of tubulins into microtubules with a percentage inhibition value of 66.39% compared with the untreated control cells. Additionally, the IC<sub>50</sub> value for compound **6a** was

recorded as 0.27  $\mu\text{M}$ . CA-4 was used as a reference compound with  $\text{IC}_{50}$  value 0.083  $\mu\text{M}$  and 88.72% tubulin inhibition. These results indicate that cytotoxicity of compound **6a** related mainly to good HDAC than  $\beta$ -tubulin polymerization inhibition activity.

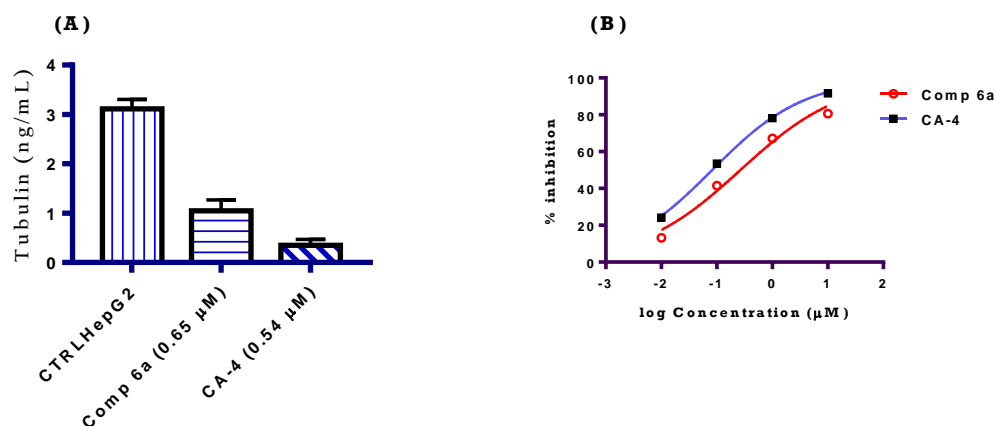


**Figure 3.** (A) Tubulin polymerization inhibition activity induced by compound **6a** compared with no treatment control cells using ELISA assay for  $\beta$ -tubulin. (B) Dose response curve for in vitro  $\beta$ -tubulin inhibitory activity of tetraamide **6a** and CA-4 against tubulin.

#### 2.2.4. Cell Cycle Analysis

Inhibition of tubulin assembly into microtubule and the antiproliferative effects are characterized by cell cycle arrest in the G2/M phase [31]. Cell cycle analysis on the most active compound was performed using FACS analysis following treatment of HepG2 cells with tetraamide derivative **6a** at its  $\text{IC}_{50}$  dose level for 48 h. As shown in Figure 4, the tested tetraamide molecule **6a** showed good ability to block cells in G2/M phase of the cells cycle (39.09%) compared with untreated control (7.28%). In addition, tetraamide derivative **6a** increase the percentage of cells at pre-G1 phase (37.51%) compared with the untreated control (1.59%). The results in this study indicate that the newly prepared tetraamide derivative **6a** cause cell cycle perturbation in the G2/M phase which is the main gauge of HDAC and tubulin inhibitors confirming the mode of action under study.

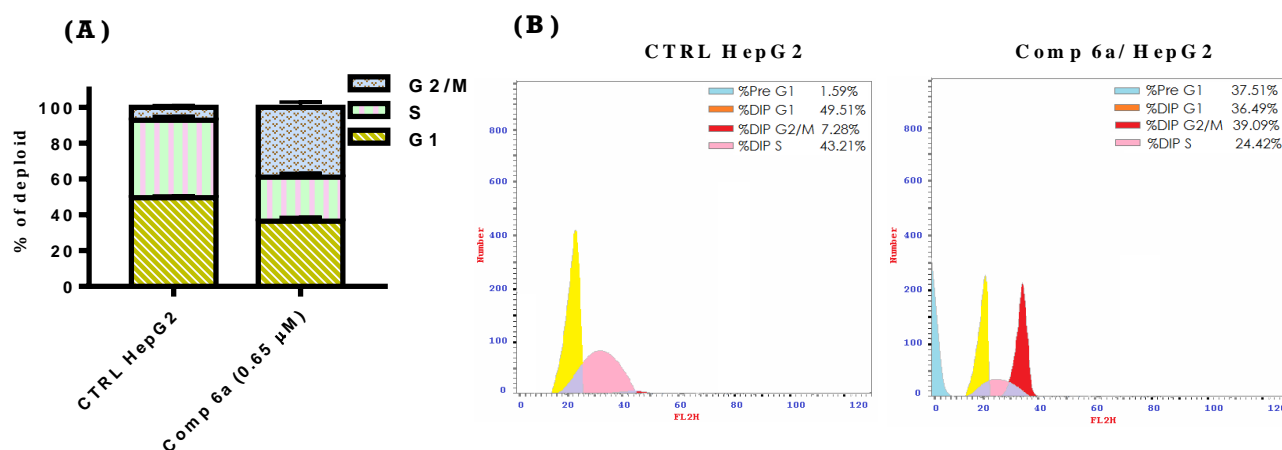


**Figure 4.** (A) Graphical representation of cell cycle analysis in HepG2 cells after 48 h of compound **6a** exposure at its  $\text{IC}_{50}$  concentration ( $\mu\text{M}$ ) compared with the untreated control. (B) Cryptograms shows cell cycle analysis after 48 h of compound **6a** exposure at its  $\text{IC}_{50}$  concentration ( $\mu\text{M}$ ) compared with the untreated control.

#### 2.2.5. Apoptosis Assay

G2/M blockade is often followed by cellular apoptosis [32]. To quantify the percentage of cellular apoptosis induced by compound **6a** in HepG2 cells, Annexin V fluorescein

isothiocyanate versus propidium iodide (PI) dual staining analysis was performed after treatment with compound **6a** at its  $IC_{50}$  concentration for 48 h. The results were presented graphically in Figure 5. From the results in Figure 5, it can be observed that the total apoptosis percentage increased in HepG2 cells (37.51%) after treatment with compound **6a** compared with the untreated control cells (1.59%). In addition the early and late apoptotic cell percentages were increased in HepG2 cells; 23.41 and 12.08%, respectively after treatment with compound **6a** compared with the untreated control cells (0.52 and 0.13%, respectively). Therefore, it can be concluded that compound **6a** can be considered as apoptotic inducer.

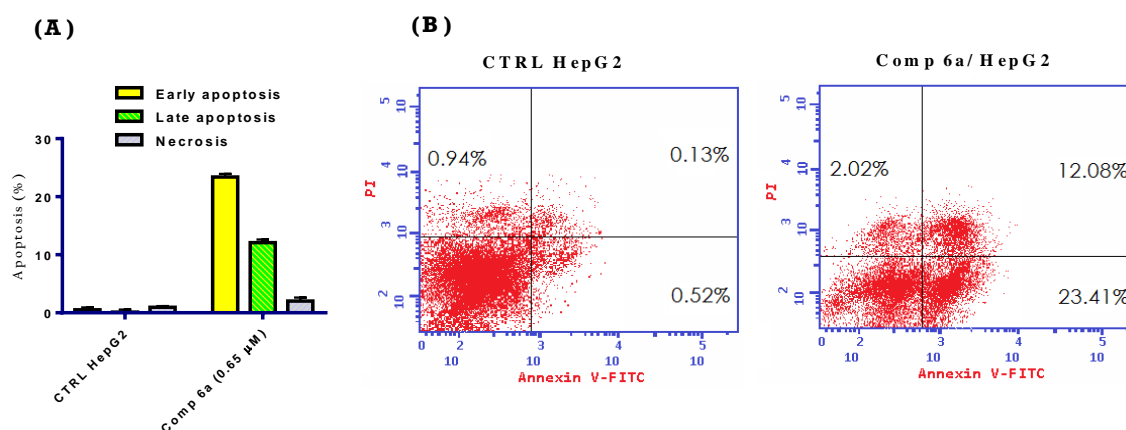


**Figure 5.** (A) Graphical representation shows the apoptosis effect by Annexin V-FITC versus PI uptake method in HepG2 cells after 48 h of compound **6a** exposure at its  $IC_{50}$  concentration ( $\mu$ M) compared with the untreated control. (B) Cryptograms show the apoptosis effect by the Annexin V-FITC versus PI uptake method in HepG2 cells after 48 h of compound **6a** exposure at its  $IC_{50}$  concentration ( $\mu$ M) compared with the untreated control.

### 2.2.6. Caspase 3/7 Assay

Further, the activation of caspase 3/7 in HepG2 cells treated with compound **6a** at its  $IC_{50}$  concentration for 48 h was carried out to investigate the apoptotic pathway mechanism. The results were presented graphically in Figure 6. From the results in Figure 6, it can be showed that the treatment of HepG2 cells with compound **6a** for 48 h the level of caspase 3/7 was increased by  $-9.73$  fold in comparison with the no treatment control. It can be concluded that compound **6a** induced apoptosis through the activation of caspase 3/7.

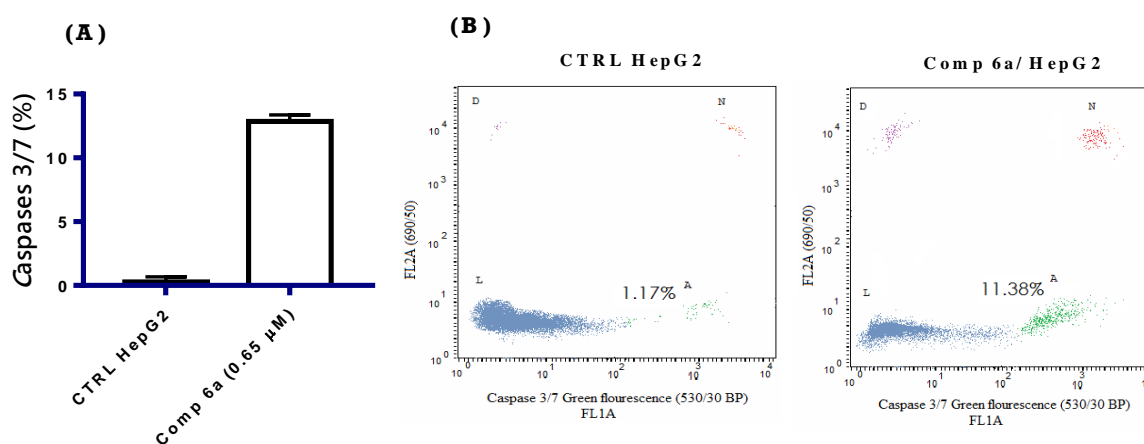


**Figure 6.** (A) Graphical representation of caspase 3/7 in HepG2 cells after 48 h of compound **6a** exposure at its  $IC_{50}$  concentration ( $\mu$ M) compared with the untreated control. (B) Cryptograms show caspase 3/7 in HepG2 cells after 48 h of compound **6a** exposure at its  $IC_{50}$  concentration ( $\mu$ M) compared with the untreated control.

### 2.2.7. Mitochondrial Membrane Potential (MMP)

To investigate the mitochondrial events,  $\Delta\Psi$  dissipation was monitored after treatment with compound **6a** with the concentration induced cytotoxicity for 48 h. Results presented in Figure 7 revealed that the  $\Delta\Psi$  was decreased from 31,559 for control untreated HepG2 cells to 13,914 when the cells were treated with the test compound. Therefore, the loss of  $\Delta\Psi$  after **6a** treatment with the concentration induced cytotoxicity concluded that the activation of caspase 3/7 may occur via mitochondrial apoptotic pathway.

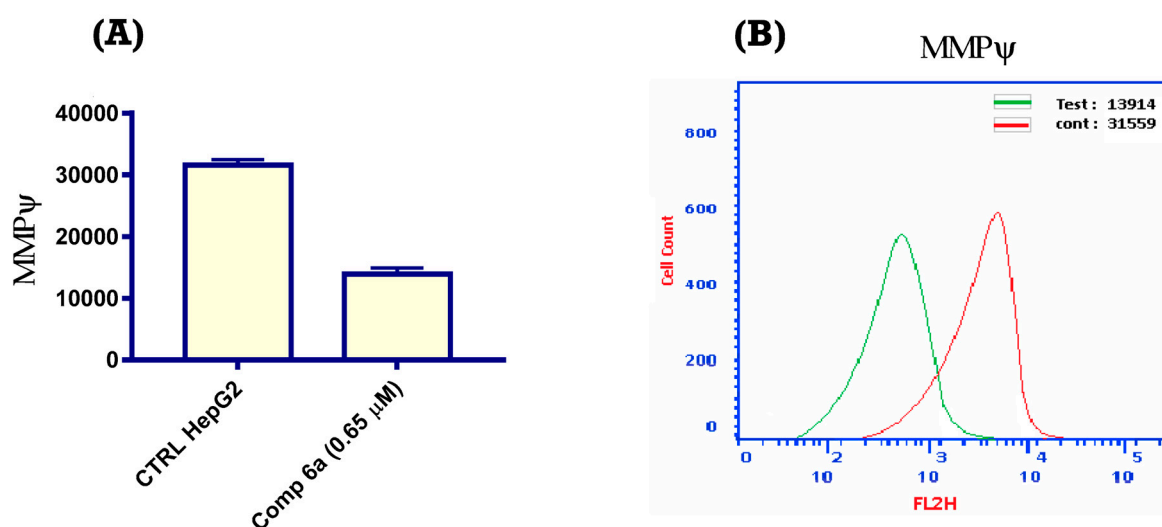


**Figure 7.** (A) Graphical representation of MMP in HepG2 cells after 48 h of compound **6a** exposure at its  $IC_{50}$  concentration ( $\mu$ M) compared with the untreated control. (B) Cryptogram shows the loss of MMP during compound **6a** treatment in in HepG2 cells after 48 h compared with the untreated control.

### 3. Conclusions

In the present study, a novel series of amide derivatives containing TMP moiety have been conveniently synthesized and characterized by  $^1H$ -NMR and  $^{13}C$ -NMR spectral analyses. The prepared amide derivatives were tested for their antiproliferative as well enzyme inhibition activity. Compounds **6a** and **6b** showed remarkable cytotoxic activity against HepG2 cells with  $IC_{50}$  values 0.65 and 0.92  $\mu$ M, respectively compared with SAHA and CA-4 as reference compounds. In addition, compound **6a** demonstrated good HDAC-tubulin dual inhibition activity as it showed better HDAC activity as well as anti-tubulin activity. Moreover, compound **6a** exhibited G2/M phase arrest and pre-G1 apoptosis as demonstrated by cell cycle analysis and Annexin V assays. Further apoptosis studies demonstrated that compound **6a** boosted the level of caspase 3/7. Caspase 3/7 activation and apoptosis induction were evidenced by decrease in mitochondrial permeability suggesting that activation of caspase 3/7 may occur via mitochondrial apoptotic pathway. In conclusion, the tetraamide analogs could be considered as lead templates for further development to obtain more potent anticancer agents.

### 4. Experimental

#### 4.1. General

Melting points, NMR spectra and elemental analyses were carried out to elucidate the chemical structure of target amide derivatives **2a–6e**. For experimental details see Section 4.1 in Supplementary Data.

## 4.2. Chemistry

### 4.2.1. General Procedure for the Preparation of N-(3-(arylamino)-1-(furan-2-yl)-3-oxoprop-1-en-2-yl)-3,4,5-trimethoxybenzamides **2a–c**

A mixture of oxazolone **1** (0.01 mol, 3.29 g) with respective aryl amine (0.01 mol) in glacial acetic acid (20 mL) was refluxed for 1–2 h. After completion of the reaction, the reaction mixture was cooled down and poured into ice/cold water and then filtered. The obtained residue was crystallized from DMF/H<sub>2</sub>O to get pure diamide compound **2a–c**.

#### N-(3-(3-chlorophenylamino)-1-(furan-2-yl)-3-oxoprop-1-en-2-yl)-3,4,5-trimethoxybenzamide (**2a**)

White powder (2.48 g, 54.33%), m.p. 248–250 °C. <sup>1</sup>H-NMR (400 MHz, DMSO-*d*<sub>6</sub>, δ ppm): 3.76 (s, 3H, OCH<sub>3</sub>), 3.88 (s, 6H, 2OCH<sub>3</sub>), 6.64 (dd, *J* = 3.4, 1.8 Hz, 1H, furan CH), 6.81 (d, *J* = 3.4 Hz, 1H, furan CH), 7.11 (s, 1H, olefinic CH), 7.14 (ddd, *J* = 8.0, 2.1, 0.8 Hz, 1H, arom.CH), 7.36 (t, *J* = 8.1 Hz, 1H, arom.CH), 7.42 (s, 2H, arom.CH), 7.66–7.71 (m, 1H, 1H, arom.CH), 7.84 (d, *J* = 1.4 Hz, 1H, furan CH), 7.91 (t, *J* = 2.0 Hz, 1H, 1H, arom.CH), 9.97 (s, 1H, NH), 10.24 (s, 1H, NH). <sup>13</sup>C-NMR (100 MHz, DMSO-*d*<sub>6</sub>, δ ppm): 56.56 (OCH<sub>3</sub>), 60.60 (2OCH<sub>3</sub>), 106.02 (C2,6 trimethoxybenzamide), 112.87 (C olefinic), 114.88 (C3 furan), 117.21 (C4 furan), 118.91 (C6 chlorophenyl), 119.95 (C2 chlorophenyl), 123.56 (C4 chlorophenyl), 128.26 (C1 trimethoxybenzamide), 129.04 (C olefinic), 130.68 (C5 chlorophenyl), 133.31 (C3 chlorophenyl), 140.96 (C4 trimethoxybenzamide), 141.16 (C1 chlorophenyl), 145.27 (C5 furan), 150.04 (C2 furan), 153.11 (C3,5 trimethoxybenzamide), 164.31 (C=O trimethoxybenzamide), 165.57 (C=O amide). Anal. Calcd. for C<sub>23</sub>H<sub>21</sub>ClN<sub>2</sub>O<sub>6</sub> (456.88): C, 60.46; H, 4.63; N, 6.13. Found: C, 60.64; H, 4.74; N, 6.02.

#### N-(3-(4-chlorophenylamino)-1-(furan-2-yl)-3-oxoprop-1-en-2-yl)-3,4,5-trimethoxybenzamide (**2b**)

White powder (2.32 g, 50.89%), m.p. 241–243 °C. <sup>1</sup>H-NMR (400 MHz, DMSO-*d*<sub>6</sub>, δ ppm): 3.75 (s, 3H, OCH<sub>3</sub>), 3.87 (s, 6H, 2OCH<sub>3</sub>), 6.63 (dd, *J* = 3.4, 1.8 Hz, 1H, furan CH), 6.80 (d, *J* = 3.4 Hz, 1H, furan CH), 7.10 (s, 1H, olefinic CH), 7.41–7.35 (m, 2H, arom.CH), 7.42 (s, 2H, arom.CH), 7.77 (d, *J* = 8.9 Hz, 2H, arom.CH), 7.83 (d, *J* = 1.5 Hz, 1H, furan CH), 9.95 (s, 1H, NH), 10.21 (s, 1H, NH). <sup>13</sup>C-NMR (100 MHz, DMSO-*d*<sub>6</sub>, δ ppm): 56.55 (OCH<sub>3</sub>), 60.59 (2OCH<sub>3</sub>), 106.02 (C2,6 trimethoxybenzamide), 112.84 (C olefinic), 114.76 (C3 furan), 117.12 (C4 furan), 122.14 (C2,6 chlorophenyl), 127.49 (C4 chlorophenyl), 128.38 (C1 trimethoxybenzamide), 128.87 (C3,5 chlorophenyl), 129.08 (C olefinic), 138.64 (C1 chlorophenyl), 140.95 (C4 trimethoxybenzamide), 145.19 (C5 furan), 150.08 (C2 furan), 153.10 (C3,5 trimethoxybenzamide), 164.14 (C=O trimethoxybenzamide), 165.54 (C=O amide). Anal. Calcd. for C<sub>23</sub>H<sub>21</sub>ClN<sub>2</sub>O<sub>6</sub> (456.88): C, 60.46; H, 4.63; N, 6.13. Found: C, 60.28; H, 4.76; N, 6.22.

#### N-(1-(furan-2-yl)-3-oxo-3-(p-tolylamino)prop-1-en-2-yl)-3,4,5-trimethoxybenzamide (**2c**)

White powder (2.51 g, 57.51%), m.p. 261–263 °C. <sup>1</sup>H-NMR (400 MHz, DMSO-*d*<sub>6</sub>, δ ppm): 2.28 (s, 3H, CH<sub>3</sub>), 3.76 (s, 3H, OCH<sub>3</sub>), 3.88 (s, 6H, 2OCH<sub>3</sub>), 6.62 (dd, *J* = 3.3, 1.7 Hz, 1H, furan CH), 6.77 (d, *J* = 3.4 Hz, 1H, furan CH), 7.12 (d, *J* = 5.3 Hz, 2H, arom.CH), 7.14 (s, 1H, olefinic CH), 7.42 (s, 2H, arom.CH), 7.61 (d, *J* = 8.4 Hz, 2H, arom.CH), 7.77–7.86 (m, 1H, furan CH), 9.91 (s, 1H, NH), 9.97 (s, 1H, NH). <sup>13</sup>C-NMR (100 MHz, DMSO-*d*<sub>6</sub>, δ ppm): 20.95 (CH<sub>3</sub>), 56.54 (OCH<sub>3</sub>), 60.59 (2OCH<sub>3</sub>), 106.01 (C2,6 trimethoxybenzamide), 112.80 (C olefinic), 114.50 (C3 furan), 117.03 (C4 furan), 120.68 (C2,6 methylphenyl), 128.61 (C1 trimethoxybenzamide), 129.22 (C olefinic), 129.33 (C3,5 methylphenyl), 132.85 (C1 methylphenyl), 137.09 (C4 methylphenyl), 140.89 (C4 trimethoxybenzamide), 145.04 (C5 furan), 150.19 (C2 furan), 153.08 (C3,5 trimethoxybenzamide), 163.79 (C=O trimethoxybenzamide), 165.54 (C=O amide). Anal. Calcd. for C<sub>24</sub>H<sub>24</sub>N<sub>2</sub>O<sub>6</sub> (436.46): C, 66.04; H, 5.54; N, 6.42. Found: C, 65.88; H, 5.68; N, 6.33.

#### 4.2.2. N-(1-(furan-2-yl)-3-(naphthalen-2-ylamino)-3-oxoprop-1-en-2-yl)-3,4,5-trimethoxybenzamide (3)

A mixture of **1** (0.01 mol, 3.29 g) with 2-naphthyl amine (0.01 mol, 1.43 g) in glacial acetic acid (20 mL) was refluxed for 3 h. After completion of the reaction, the reaction mixture was cooled down, poured into ice/cold water and then filtered. The obtained residue was crystallized from DMF/H<sub>2</sub>O to get pure diamide compound **3**.

Buff powder (2.35 g, 49.79%), m.p. 270–272 °C. <sup>1</sup>H-NMR (400 MHz, DMSO-*d*<sub>6</sub>, δ ppm): 3.75 (s, 3H, OCH<sub>3</sub>), 3.89 (s, 6H, 2OCH<sub>3</sub>), 6.65 (dd, *J* = 3.1, 1.8 Hz, 1H, furan CH), 6.84 (d, *J* = 3.4 Hz, 1H, furan CH), 7.30 (s, 1H, olefinic CH), 7.47 (s, 2H, arom.CH), 7.51–7.60 (m, 4H, arom.CH), 7.80–7.89 (m, 2H, furan CH), 7.93–8.01 (m, 1H, furan CH), 8.05–8.14 (m, 1H, arom.CH), 10.03 (s, 1H, NH), 10.15 (s, 1H, NH). <sup>13</sup>C-NMR (100 MHz, DMSO-*d*<sub>6</sub>, δ ppm): 56.58 (OCH<sub>3</sub>), 60.60 (2OCH), 106.13 (C2,6 trimethoxybenzamide), 112.85 (C olefinic), 114.83 (C3 furan), 117.85 (C4 furan), 123.97 (C1 naphthyl), 124.19 (C3 naphthyl), 125.93 (C6 naphthyl), 126.22 (C8 naphthyl), 126.47 (C7 naphthyl), 126.54 (C5 naphthyl), 128.20 (C4'' naphthyl), 128.38 (C1 trimethoxybenzamide), 129.43 (C olefinic), 129.68 (C4 naphthyl), 134.17 (C8'' naphthyl), 134.43 (C2 naphthyl), 140.88 (C4 trimethoxybenzamide), 145.24 (C5 furan), 150.23 (C2 furan), 153.06 (C3,5 trimethoxybenzamide), 164.67 (C=O trimethoxybenzamide), 166.01 (C=O amide). Anal. Calcd. for C<sub>27</sub>H<sub>24</sub>N<sub>2</sub>O<sub>6</sub> (472.49): C, 68.63; H, 5.12; N, 5.93. Found: C, 68.69; H, 5.22; N, 6.01.

#### 4.2.3. General Procedure for the Preparation of N-(3-(2-(4-Aroyl)hydrazinyl)-1-(furan-2-yl)-3-oxoprop-1-en-2-yl)-3,4,5-trimethoxybenzamides (4a,b)

A mixture of oxazolone **1** (0.01 mol, 3.29 g) with respective aryl carbohydrazide (0.01 mol) in pure ethanol was refluxed for 4–5 h. After completion of the reaction, the reaction mixture was cooled down and then filtered. The buff residue that formed was crystallized from ethanol (70%) as buff crystals.

#### N-(1-(furan-2-yl)-3-(2-(3-hydroxybenzoyl)hydrazinyl)-3-oxoprop-1-en-2-yl)-3,4,5-trimethoxybenzamide (4a)

Buff powder (2.67 g, 55.81%), m.p. 235–237 °C. <sup>1</sup>H-NMR (400 MHz, DMSO-*d*<sub>6</sub>, δ ppm): 3.75 (s, 3H, OCH<sub>3</sub>), 3.88 (s, 6H, 2OCH<sub>3</sub>), 6.62 (dd, *J* = 3.3, 1.8 Hz, 1H, furan CH), 6.78 (d, *J* = 3.4 Hz, 1H, furan CH), 6.93–7.00 (m, 1H, arom.CH), 7.25 (s, 1H, olefinic CH), 7.26–7.31 (m, 2H, arom.CH), 7.34 (d, *J* = 7.8 Hz, 1H, arom.CH), 7.41 (s, 2H, arom.CH), 7.81 (d, *J* = 1.4 Hz, 1H, furan CH), 9.71 (s, 1H, OH), 9.85 (s, 1H, NH), 10.15 (s, 1H, NH), 10.35 (s, 1H, NH). <sup>13</sup>C-NMR (100 MHz, DMSO-*d*<sub>6</sub>, δ ppm): 56.52 (OCH<sub>3</sub>), 60.61 (2OCH<sub>3</sub>), 106.04 (C2,6 trimethoxybenzamide), 112.90 (C olefinic), 114.87 (C3 furan), 115.09 (C2 hydroxyphenyl), 118.50 (C4 furan), 119.03 (C4 hydroxyphenyl), 119.19 (C6 hydroxyphenyl), 126.25 (C1 trimethoxybenzamide), 129.41 (C olefinic), 130.01 (C5 hydroxyphenyl), 134.43 (C1 hydroxyphenyl), 140.77 (C4 trimethoxybenzamide), 145.31 (C5 furan), 149.92 (C2 furan), 152.99 (C3,5 trimethoxybenzamide), 157.71 (C3 hydroxyphenyl), 164.63 (C=O amide), 165.93 (C=O amide), 166.30 (C=O trimethoxybenzamide). Anal. Calcd. for C<sub>24</sub>H<sub>23</sub>N<sub>3</sub>O<sub>8</sub> (481.45): C, 59.87; H, 4.82; N, 8.73. Found: C, 60.03; H, 4.69; N, 8.56.

#### N-(1-(furan-2-yl)-3-(2-isonicotinoylhydrazinyl)-3-oxoprop-1-en-2-yl)-3,4,5-trimethoxybenzamide (4b)

Pale buff powder (2.44 g, 52.24%), m.p. 228–230 °C. <sup>1</sup>H-NMR (400 MHz, DMSO-*d*<sub>6</sub>, δ ppm): 3.75 (s, 3H, OCH<sub>3</sub>), 3.88 (s, 6H, 2OCH<sub>3</sub>), 6.63 (dd, *J* = 3.3, 1.7 Hz, 1H, furan CH), 6.80 (d, *J* = 3.4 Hz, 1H, furan CH), 7.25 (s, 1H, olefinic CH), 7.41 (s, 2H, arom.CH), 7.82 (d, *J* = 1.4 Hz, 1H, furan CH), 7.83 (s, 2H, arom.CH), 8.78 (d, *J* = 5.3 Hz, 2H, arom.CH), 9.90 (s, 1H, NH), 10.32 (s, 1H, NH), 10.80 (s, 1H, NH). <sup>13</sup>C-NMR (100 MHz, DMSO-*d*<sub>6</sub>, δ ppm): 56.54 (OCH<sub>3</sub>), 60.59 (2OCH<sub>3</sub>), 106.10 (C2,6 trimethoxybenzamide), 112.89 (C olefinic), 115.09 (C3

furan), 118.94 (C4 furan), 121.83 (C3,5 pyridyl), 126.40 (C1 trimethoxybenzamide), 129.40 (C olefinic), 140.07 (C4 pyridyl), 140.82 (C4 trimethoxybenzamide), 145.38 (C5 furan), 149.95 (C2 furan), 150.87 (C2,6 pyridyl), 153.01 (C3,5 trimethoxybenzamide), 164.48 (C=O amide), 164.52 (C=O amide), 165.81 (C=O trimethoxybenzamide). Anal. Calcd. for C<sub>23</sub>H<sub>22</sub>N<sub>4</sub>O<sub>7</sub> (466.44): C, 59.22; H, 4.75; N, 12.01. Found: C, 58.97; H, 4.87; N, 11.93.

#### 4.2.4. General Procedure for the Synthesis of N-(4-(2-(3-(furan-2-yl)-2-(3,4,5-trimethoxybenzamido)acryloyl)hydrazinyl)phenyl)nicotinamide (5)

N-[4-(hydrazinyl)phenyl]nicotinamide (0.01 mol, 2.56 g) was added to a suspension of compound **1** (0.01 mol, 3.29 g) in dry DMF (20 mL) containing catalytic amount glacial acetic acid (10 drops) and the mixture was refluxed for 6 h. After completion of the reaction, the reaction mixture was then cooled and poured into ice/cold water. The residue was purified by crystallization from pure ethanol to furnish pure compound **5**.

Pale yellow powder (3.49 g, 59.66%), m.p. 217–219 °C. <sup>1</sup>H-NMR (400 MHz, DMSO-*d*<sub>6</sub>, δ ppm): 3.75 (s, 3H, OCH<sub>3</sub>), 3.88 (s, 6H, 2OCH<sub>3</sub>), 6.62 (dd, *J* = 3.4, 1.8 Hz, 1H, furan CH), 6.79 (d, *J* = 3.4 Hz, 1H, furan CH), 7.25 (s, 1H, olefinic CH), 7.41 (s, 2H, arom.CH), 7.60 (dd, *J* = 7.5, 4.8 Hz, 1H, arom.CH), 7.82 (d, *J* = 1.4 Hz, 1H, furan CH), 7.90 (d, *J* = 8.9 Hz, 2H, arom.CH), 7.96 (d, *J* = 8.8 Hz, 2H, arom.CH), 8.32 (dt, *J* = 8.0, 1.9 Hz, 1H, arom.CH), 8.75–8.83 (m, 1H, arom.CH), 9.13 (s, 1H, arom.CH), 9.87 (s, 1H, NH), 10.18 (s, 1H, NH), 10.40 (s, 1H, NH), 10.68 (s, 1H, NH). <sup>13</sup>C-NMR (100 MHz, DMSO-*d*<sub>6</sub>, δ ppm): 56.54 (OCH<sub>3</sub>), 60.58 (2OCH<sub>3</sub>), 106.10 (C2,6 trimethoxybenzamide), 112.86 (C olefinic), 114.88 (C3 furan), 118.78 (C4 furan), 120.00 (C3,5 phenyl), 124.01 (C5 pyridyl), 126.66 (C1 trimethoxybenzamide), 128.24 (C1 phenyl), 128.82 (C2,6 phenyl), 129.48 (C olefinic), 130.87 (C3 pyridyl), 136.04 (C4 pyridyl), 140.78 (C4 trimethoxybenzamide), 142.38 (C4 phenyl), 145.27 (C5 furan), 149.21 (C3 furan), 150.02 (C6 pyridyl), 152.77 (C2 pyridyl), 152.99 (C3,5 trimethoxybenzamide), 164.61 (C=O amide), 164.90 (C=O amide), 165.45 (C=O amide), 165.75 (C=O trimethoxybenzamide). Anal. Calcd. for C<sub>30</sub>H<sub>27</sub>N<sub>5</sub>O<sub>8</sub> (585.56): C, 61.53; H, 4.65; N, 11.96. Found: C, 61.66; H, 4.73; N, 11.88.

#### 4.2.5. General Procedure for the Synthesis of N-((1Z)-3-(2-(3-(aryl)-2-(3,4,5-trimethoxybenzamido)acryloyl)hydrazinyl)-1-(furan-2-yl)-3-oxoprop-1-en-2-yl)-3,4,5-trimethoxybenzamide (6a–e)

A mixture of oxazolone **1** (0.01 mol 3.29 g) with respective acrylic acid hydrazide (0.01 mol) in DMF (20 mL) and catalytic amount glacial acetic acid (10 drops) was refluxed for 6–8 h. After completion of the reaction the reaction mixture was then cooled and poured into ice/cold water. The formed precipitate was crystallized from DMF/H<sub>2</sub>O to afford pure compound **6a–e**.

N-((1Z)-3-(2-(3-(4-chlorophenyl)-2-(3,4,5-trimethoxybenzamido)acryloyl)hydrazinyl)-1-(furan-2-yl)-3-oxoprop-1-en-2-yl)-3,4,5-trimethoxybenzamide (**6a**)

White powder (3.72 g, 50.54%), m.p. 209–211 °C. <sup>1</sup>H-NMR (400 MHz, DMSO-*d*<sub>6</sub>, δ ppm): 3.74 (s, 3H, OCH<sub>3</sub>), 3.75 (s, 3H, OCH<sub>3</sub>), 3.85 (s, 6H, 2OCH<sub>3</sub>), 3.87 (s, 6H, 2OCH<sub>3</sub>), 6.61 (dd, *J* = 3.2, 1.7 Hz, 1H, furan CH), 6.76 (d, *J* = 3.4 Hz, 1H, furan CH), 7.22 (s, 1H, olefinic CH), 7.25 (s, 1H, olefinic CH), 7.35 (s, 2H, arom.CH), 7.39 (s, 2H, arom.CH), 7.47 (d, *J* = 8.6 Hz, 2H, arom.CH), 7.62 (d, *J* = 8.6 Hz, 2H, arom.CH), 7.81 (d, *J* = 1.3 Hz, 1H, furan CH), 9.81 (s, 1H, NH), 9.93 (s, 1H, NH), 10.20 (s, 1H, NH), 10.26 (s, 1H, NH). <sup>13</sup>C-NMR (100 MHz, DMSO-*d*<sub>6</sub>, δ ppm): 56.53 (4OCH<sub>3</sub>), 60.57 (2OCH<sub>3</sub>), 106.06 (C2,6 trimethoxybenzamide), 106.08 (C2,6 trimethoxybenzamide), 112.85 (C olefinic), 114.74 (C3 furan), 118.74 (C4 furan), 119.68 (C olefinic), 126.64 (C1 trimethoxybenzamide), 128.66 (C1 trimethoxybenzamide), 129.11 (C3,5 chlorophenyl), 129.47 (C olefinic), 130.18 (C olefinic), 131.57 (C2,6 chlorophenyl), 133.48 (C1 chlorophenyl), 133.69 (C4 chlorophenyl), 140.76 (C4 trimethoxybenzamide), 140.88 (C4 trimethoxybenzamide), 145.19 (C5 furan), 150.03 (C2 furan), 152.99 (C3,5 trimethoxybenzamide), 153.00 (C3,5 trimethoxybenzamide), 164.24 (C=O amide), 164.75 (C=O amide),

165.62 (C=O trimethoxybenzamide), 165.77 (C=O trimethoxybenzamide). Anal. Calcd. for  $C_{36}H_{35}ClN_4O_{11}$  (735.14): C, 58.82; H, 4.80; N, 7.62. Found: C, 59.02; H, 4.88; N, 7.43.

N-((1Z)-3-(2-(3-(4-cyanophenyl)-2-(3,4,5-trimethoxybenzamido)acryloyl)hydrazinyl)-1-(furan-2-yl)-3-oxoprop-1-en-2-yl)-3,4,5-trimethoxybenzamide (**6b**)

Yellow powder (4.43 g, 61.03%), m.p. 223–225 °C.  $^1H$ -NMR (400 MHz, DMSO- $d_6$ ,  $\delta$  ppm): 3.73 (s, 3H, OCH<sub>3</sub>), 3.74 (s, 3H, OCH<sub>3</sub>), 3.84 (s, 6H, 2OCH<sub>3</sub>), 3.86 (s, 6H, 2OCH<sub>3</sub>), 6.60 (dd,  $J$  = 3.4, 1.8 Hz, 1H, furan CH), 6.76 (d,  $J$  = 3.4 Hz, 1H, furan CH), 7.22 (s, olefinic CH), 7.25 (s, olefinic CH), 7.33 (s, 2H, arom.CH), 7.39 (s, 2H, arom.CH), 7.75 (d,  $J$  = 8.4 Hz, 2H, arom.CH), 7.80 (d,  $J$  = 1.4 Hz, 1H, furan CH), 7.86 (d,  $J$  = 8.4 Hz, 2H, arom.CH), 9.81 (s, 1H, NH), 10.04 (s, 1H, NH), 10.23 (s, 1H, NH), 10.36 (s, 1H, NH).  $^{13}C$ -NMR (100 MHz, DMSO- $d_6$ ,  $\delta$  ppm): Anal. Calcd. for  $C_{37}H_{35}N_5O_{11}$  (725.70): C, 61.24; H, 4.86; N, 9.65. Found: C, 61.06; H, 4.98; N, 9.58.

N-((1Z)-3-(2-(3-(4-(dimethylamino)phenyl)-2-(3,4,5-trimethoxybenzamido)acryloyl)hydrazinyl)-1-(furan-2-yl)-3-oxoprop-1-en-2-yl)-3,4,5-trimethoxybenzamide (**6c**)

Orange powder (3.77 g, 50.73%), m.p. 215–217 °C.  $^1H$ -NMR (400 MHz, DMSO- $d_6$ ,  $\delta$  ppm): 2.93 (s, 6H, 2CH<sub>3</sub>), 3.75 (s, 6H, 2OCH<sub>3</sub>), 3.87 (s, 12H, 4OCH<sub>3</sub>), 6.60 (s, 1H, furan CH), 6.69 (d,  $J$  = 8.7 Hz, 2H, arom.CH), 6.74 (d,  $J$  = 3.0 Hz, 1H, furan CH), 7.21 (s, 1H, olefinic CH), 7.28 (s, 1H, olefinic CH), 7.39 (s, 2H, arom.CH), 7.40 (s, 2H, arom.CH), 7.47 (d,  $J$  = 8.7 Hz, 2H, arom.CH), 7.80 (s, 1H, furan CH), 9.75 (s, 1H, NH), 9.80 (s, 1H, NH), 9.97 (s, 2H, 2NH).  $^{13}C$ -NMR (100 MHz, DMSO- $d_6$ ,  $\delta$  ppm): 40.40 (2CH<sub>3</sub>), 56.52 (4OCH<sub>3</sub>), 60.57 (2OCH<sub>3</sub>), 106.03 (2C<sub>2,6</sub> trimethoxybenzamide), 112.14 (C<sub>3,5</sub> dimethylaminophenyl), 112.83 (C olefinic), 114.60 (C<sub>3</sub> furan), 118.55 (C<sub>4</sub> furan), 121.74 (C olefinic), 124.28 (C<sub>1</sub> dimethylaminophenyl), 126.78 (C olefinic), 129.50 (C<sub>1</sub> trimethoxybenzamide), 129.60 (C<sub>1</sub> trimethoxybenzamide), 131.70 (C<sub>2,6</sub> dimethylaminophenyl), 131.94 (C olefinic), 140.65 (C<sub>4</sub> trimethoxybenzamide), 140.74 (C<sub>4</sub> trimethoxybenzamide), 145.11 (C<sub>5</sub> furan), 150.09 (C<sub>2</sub> furan), 151.08 (C<sub>4</sub> dimethylaminophenyl), 152.97 (2C<sub>3,5</sub> trimethoxybenzamide), 164.18 (C=O amide), 165.19 (C=O amide), 165.59 (C=O trimethoxybenzamide), 165.66 (C=O trimethoxybenzamide). Anal. Calcd. for  $C_{38}H_{41}N_5O_{11}$  (743.76): C, 61.36; H, 5.56; N, 9.42. Found: C, 61.47; H, 5.63; N, 9.31.

N-(3-(2-((Z)-3-(furan-2-yl)-2-(3,4,5-trimethoxybenzamido)acryloyl)hydrazinyl)-1-(4-methoxyphenyl)-3-oxoprop-1-en-2-yl)-3,4,5-trimethoxybenzamide (**6d**)

Red powder (3.61 g, 49.41%), m.p. 206–208 °C.  $^1H$ -NMR (400 MHz, DMSO- $d_6$ ,  $\delta$  ppm): 3.74 (s, 6H, 2OCH<sub>3</sub>), 3.77 (s, 3H, OCH<sub>3</sub>), 3.86 (s, 6H, 2OCH<sub>3</sub>), 3.87 (s, 6H, 2OCH<sub>3</sub>), 6.59–6.64 (m, 1H, furan CH), 6.75 (d,  $J$  = 3.4 Hz, 1H, furan CH), 6.97 (d,  $J$  = 8.8 Hz, 2H, arom.CH), 7.22 (s, 1H, olefinic CH), 7.29 (s, 1H, olefinic CH), 7.38 (s, 2H, arom.CH), 7.39 (s, 2H, arom.CH), 7.58 (d,  $J$  = 8.8 Hz, 2H, arom.CH), 7.81 (s, 1H, furan CH), 9.80 (s, 1H, NH), 9.83 (s, 1H, NH), 10.12 (s, 1H, NH), 10.15 (s, 1H, NH).  $^{13}C$ -NMR (100 MHz, DMSO- $d_6$ ,  $\delta$  ppm): 55.70 (OCH<sub>3</sub>), 56.52 (4OCH<sub>3</sub>), 60.57 (2OCH<sub>3</sub>), 106.04 (2C<sub>2,6</sub> trimethoxybenzamide), 112.82 (C olefinic), 114.57 (C<sub>3,5</sub> methoxyphenyl), 114.71 (C<sub>3</sub> furan), 118.71 (C<sub>4</sub> furan), 126.66 (C olefinic), 127.13 (C<sub>1</sub> methoxyphenyl), 127.15 (C<sub>1</sub> trimethoxybenzamide), 129.35 (C olefinic), 129.47 (C<sub>1</sub> trimethoxybenzamide), 130.53 (C olefinic), 131.51 ( ), 131.74 (C<sub>2,6</sub> methoxyphenyl), 140.75 (2C<sub>4</sub> trimethoxybenzamide), 145.17 (C<sub>5</sub> furan), 150.03 (C<sub>2</sub> furan), 152.98 (2C<sub>3,5</sub> trimethoxybenzamide), 160.23 (C<sub>4</sub> methoxyphenyl), 163.98 (C=O amide), 164.24 (C=O amide), 165.05 (C=O trimethoxybenzamide), 165.76 (C=O trimethoxybenzamide). Anal. Calcd. for  $C_{37}H_{38}N_4O_{12}$  (730.72): C, 60.82; H, 5.24; N, 7.67. Found: C, 61.00; H, 5.37; N, 7.51.

N-(3-(2-((Z)-3-(furan-2-yl)-2-(3,4,5-trimethoxybenzamido)acryloyl)hydrazinyl)-3-oxo-1-(3,4,5-trimethoxyphenyl)prop-1-en-2-yl)-3,4,5-trimethoxybenzamide (**6e**)

Orange powder (3.68 g, 46.51%), m.p. 212–214 °C. <sup>1</sup>H-NMR (400 MHz, DMSO-*d*<sub>6</sub>, δ ppm): 3.65 (s, 6H, 2OCH<sub>3</sub>), 3.67 (s, 3H, OCH<sub>3</sub>), 3.74 (s, 3H, OCH<sub>3</sub>), 3.75 (s, 3H, OCH<sub>3</sub>), 3.84 (s, 6H, 2OCH<sub>3</sub>), 3.87 (s, 6H, 2OCH<sub>3</sub>), 6.59–6.65 (m, 1H, furan CH), 6.76 (d, *J* = 3.4 Hz, 1H, furan CH), 7.00 (s, 2H, arom.CH), 7.24 (s, 1H, olefinic CH), 7.36 (s, 1H, olefinic CH), 7.40 (s, 2H, arom.CH), 7.42 (s, 2H, arom.CH), 7.81 (s, 1H, furan CH), 9.81 (s, 1H, NH), 9.89 (s, 1H, NH), 10.21 (s, 2H, 2NH). <sup>13</sup>C-NMR (100 MHz, DMSO-*d*<sub>6</sub>, δ ppm): 56.07 (2OCH<sub>3</sub>), 56.53 (4OCH<sub>3</sub>), 60.52 (OCH<sub>3</sub>), 60.57 (OCH<sub>3</sub>), 60.63 (OCH<sub>3</sub>), 106.02 (C2,6 trimethoxybenzamide), 106.06 (C2,6 trimethoxybenzamide), 107.68 (C2,6 trimethoxyphenyl), 112.85 (C olefinic), 114.73 (C3 furan), 118.78 (C4 furan), 126.67 (C olefinic), 128.51 (C1 trimethoxyphenyl), 129.26 (C1 trimethoxybenzamide), 129.51 (C1 trimethoxybenzamide), 129.76 (C olefinic), 131.18 (C olefinic), 138.62 (C4 trimethoxyphenyl), 140.76 (C4 trimethoxybenzamide), 140.84 (C4 trimethoxybenzamide), 145.18 (C5 furan), 150.05 (C2 furan), 152.94 (C3,5 trimethoxyphenyl), 152.99 (C3,5 trimethoxybenzamide), 153.05 (C3,5 trimethoxybenzamide), 164.20 (C=O amide), 164.75 (C=O amide), 165.64 (C=O trimethoxybenzamide), 165.74 (C=O trimethoxybenzamide). Anal. Calcd. for C<sub>39</sub>H<sub>42</sub>N<sub>4</sub>O<sub>14</sub> (790.77): C, 59.24; H, 5.35; N, 7.09. Found: C, 59.41; H, 5.52; N, 6.90.

### 4.3. Biological Studies

#### 4.3.1. Cytotoxic Activity Evaluation

Cytotoxic activity was carried out using MTT colorimetric antiproliferative assay to investigate the effect of the prepared molecules on HepG2 as well as HL-7702 cell lines. See Section 4.3.1 in Supplementary Data.

#### 4.3.2. In Vitro HDAC Inhibition Assay

The in vitro HDAC inhibitory activities of compound **6a** and SAHA against two HDAC isoforms (HDAC1, 2) were measured using ELISA assay kits {Mybiosource, Inc. [#MBS2020012 and #MBS2510971]} according to manufacturer's directions. See Section 4.3.2 in Supplementary Data.

#### 4.3.3. In Vitro Tubulin Inhibition Assay

Compound **6a** and CA-4 were evaluated for their tubulin inhibitory activity according to manufacturer's instructions using # abcam Human Beta-tubulin sim-plestep ELISA Kit ab245722. See Section 4.3.3 in Supplementary Data.

#### 4.3.4. Cell Cycle Analysis

Cell cycle analysis in HepG2 cells was investigated using fluorescent Annexin V-FITC/ PI detection kit (*BioVision* EZCell™ Cell Cycle Analysis Kit Catalog #K920) by flow cytometry assay. See Section 4.3.4 in Supplementary Data.

#### 4.3.5. Apoptosis Assay

Apoptosis in HepG2 cells was investigated using fluorescent Annexin V-FITC/ PI detection kit (*BioVision* Annexin V-FITC Apoptosis Detection Kit, Catalog #: K101) by flow cytometry assay. See Section 4.3.5 in Supplementary Data.

#### 4.3.6. Caspase 3/7 Assay

Caspase 3/7 in HepG2 cells was investigated using CellEvent® Caspase 3/7 Green Detection Flow Cytometry Assay Kit according to manufacturer's directions. See Section 4.3.6 in Supplementary Data.

#### 4.3.7. Mitochondrial Membrane Potential (MMP) Assay

MMP was measured by FACS analysis using abcam ab113852TMRE Mitochondrial Membrane Potential Assay Kit according to manufacturer's directions. See Section 4.3.7 in Supplementary Data.

**Supplementary Materials:** The following supporting information can be downloaded at: <https://www.mdpi.com/article/10.3390/molecules27123960/s1>, Figure S1: <sup>1</sup>H-NMR spectrum of compound **2a**, Figure S2: <sup>13</sup>C-NMR spectrum of compound **2a**, Figure S3: <sup>1</sup>H-NMR spectrum of compound **2b**, Figure S4: <sup>13</sup>C-NMR spectrum of compound **2b**, Figure S5: <sup>1</sup>H-NMR spectrum of compound **2c**, Figure S6: <sup>13</sup>C-NMR spectrum of compound **2c**, Figure S7: <sup>1</sup>H-NMR spectrum of compound **3**, Figure S8: <sup>13</sup>C-NMR spectrum of compound **3**, Figure S9: <sup>1</sup>H-NMR spectrum of compound **4a**, Figure S10: <sup>13</sup>C-NMR spectrum of compound **4a**, Figure S11: <sup>1</sup>H-NMR spectrum of compound **4b**, Figure S12: <sup>13</sup>C-NMR spectrum of compound **4b**, Figure S13: <sup>1</sup>H-NMR spectrum of compound **5**, Figure S14: <sup>13</sup>C-NMR spectrum of compound **5**, Figure S15: <sup>1</sup>H-NMR spectrum of compound **6a**, Figure S16: <sup>13</sup>C-NMR spectrum of compound **6a**, Figure S17: <sup>1</sup>H-NMR spectrum of compound **6b**, Figure S18: <sup>1</sup>H-NMR spectrum of compound **6c**, Figure S19: <sup>13</sup>C-NMR spectrum of compound **6c**, Figure S20: <sup>1</sup>H-NMR spectrum of compound **6d**, Figure S21: <sup>13</sup>C-NMR spectrum of compound **6d**, Figure S22: <sup>1</sup>H-NMR spectrum of compound **6e**, Figure S23: <sup>13</sup>C-NMR spectrum of compound **6e**. Section 4.1. Chemistry: General. Section 4.3. Biological studies.

**Author Contributions:** Conceptualization, I.Z. and T.A.-W.; methodology, T.A.-W., F.A., O.A.A.A., A.H.A.A. and I.Z.; data curation, A.A., E.F., S.A., S.N.A.B., A.I.M.K. and I.Z.; software, A.I.M.K., S.N.A.B. and I.Z.; resources, T.A.-W., A.A., A.H.A.A., F.A., S.A. and I.Z.; supervision, I.Z.; funding acquisition, T.A.-W., A.A., F.A., O.A.A.A. and S.A.; original draft preparation, I.Z. and T.A.-W.; Writing, review, and editing, all authors. All authors have read and agreed to the published version of the manuscript.

**Funding:** The authors extend their appreciation to the Princess Nourah bint Abdulrahman University Researchers Supporting Project number (PNURSP2022R25), Princess Nourah bint Abdulrahman University, Riyadh, Saudi Arabia & Deanship of Scientific Research at Taif University for funding this work through Taif University Researchers Supporting Project number (TURSP-2020/197), Taif University, Taif, Saudi Arabia.

**Institutional Review Board Statement:** Not applicable.

**Informed Consent Statement:** Not applicable.

**Data Availability Statement:** Not applicable.

**Acknowledgments:** The authors extend their appreciation to the Princess Nourah bint Abdulrahman University Researchers Supporting Project number (PNURSP2022R25), Princess Nourah bint Abdulrahman University, Riyadh, Saudi Arabia & Deanship of Scientific Research at Taif University for funding this work through Taif University Researchers Supporting Project number (TURSP-2020/197), Taif University, Taif, Saudi Arabia.

**Conflicts of Interest:** The authors declare no conflict of interest.

**Sample Availability:** The authors confirm that the data supporting the findings of this study are available within the article.

## References

1. Liu, Q.; Zhang, B.; Wang, Y.; Wang, X.; Gou, S. Discovery of phthalazino[1,2-b]-quinazolinone derivatives as multi-target HDAC inhibitors for the treatment of hepatocellular carcinoma via activating the p53 signal pathway. *Eur. J. Med. Chem.* **2021**, *229*, 114058. [[CrossRef](#)] [[PubMed](#)]
2. Chen, C.; Li, X.; Zhao, H.; Liu, M.; Du, J.; Zhang, J.; Yang, X.; Hou, X.; Fang, H. Discovery of DNA-Targeting HDAC Inhibitors with Potent Antitumor Efficacy In Vivo That Trigger Antitumor Immunity. *J. Med. Chem.* **2022**, *65*, 3667–3683. [[CrossRef](#)] [[PubMed](#)]
3. Chen, J.-S.; Chou, C.-H.; Wu, Y.-H.; Yang, M.-H.; Chu, S.-H.; Chao, Y.-S.; Chen, C.-N. CC-01 (chidamide plus celecoxib) modifies the tumor immune microenvironment and reduces tumor progression combined with immune checkpoint inhibitor. *Sci. Rep.* **2022**, *12*, 1–18. [[CrossRef](#)]
4. Dhiman, A.; Sharma, R.; Singh, R.K. Target-based anticancer indole derivatives and insight into structure—Activity relationship: A mechanistic review update (2018–2021). *Acta Pharm. Sin. B*, 2022; *In Press*.

5. Wang, Y.-Q.; Wang, P.-Y.; Wang, Y.-T.; Yang, G.-F.; Zhang, A.; Miao, Z.-H. An Update on Poly(ADP-ribose)polymerase-1 (PARP-1) Inhibitors: Opportunities and Challenges in Cancer Therapy. *J. Med. Chem.* **2016**, *59*, 9575–9598. [[CrossRef](#)]
6. Tian, Y.; Xie, Z.; Liao, C. Design, synthesis and anticancer activities of novel dual poly(ADP-ribose) polymerase-1/histone deacetylase-1 inhibitors. *Bioorg. Med. Chem. Lett.* **2020**, *30*, 127036. [[CrossRef](#)] [[PubMed](#)]
7. Yan, J.; Xu, Y.; Jin, X.; Zhang, Q.; Ouyang, F.; Han, L.; Zhan, M.; Li, X.; Liang, B.; Huang, X. Structure modification and biological evaluation of indole-chalcone derivatives as anti-tumor agents through dual targeting tubulin and TrxR. *Eur. J. Med. Chem.* **2021**, *227*, 113897. [[CrossRef](#)]
8. Dushanan, R.; Weerasinghe, S.; Dissanayake, D.P.; Senthiliniy, R. Cracking a cancer code histone deacetylation in epigenetic: The implication from molecular dynamics simulations on efficacy assessment of histone deacetylase inhibitors. *J. Biomol. Struct. Dyn.* **2020**, *40*, 2352–2368. [[CrossRef](#)]
9. Doke, M.; Pendyala, G.; Samikkannu, T. Psychostimulants and opioids differentially influence the epigenetic modification of histone acetyltransferase and histone deacetylase in astrocytes. *PLoS ONE* **2021**, *16*, e0252895. [[CrossRef](#)]
10. Moreno-Yruela, C.; Zhang, D.; Wei, W.; Bæk, M.; Liu, W.; Gao, J.; Danková, D.; Nielsen, A.L.; Bolding, J.E.; Yang, L.; et al. Class I histone deacetylases (HDAC1–3) are histone lysine deacetylases. *Sci. Adv.* **2022**, *8*, eabi6696. [[CrossRef](#)]
11. Wang, K.; Tang, R.; Wang, S.; Xiong, Y.; Wang, W.; Chen, G.; Zhang, K.; Li, P.; Tang, Y.-D. Isoform-Selective HDAC Inhibitor Mocetinostat (MGCD0103) Alleviates Myocardial Ischemia/Reperfusion Injury Via Mitochondrial Protection Through the HDACs/CREB/PGC-1 $\alpha$  Signaling Pathway. *J. Cardiovasc. Pharmacol.* **2021**, *79*, 217–228. [[CrossRef](#)]
12. Kowluru, R.A.; Mohammad, G. Epigenetic modifications in diabetes. *Metabolism* **2022**, *126*, 154920. [[CrossRef](#)] [[PubMed](#)]
13. Palamaris, K.; Moutafi, M.; Gakiopoulou, H.; Theocharis, S. Histone Deacetylase (HDAC) Inhibitors: A Promising Weapon to Tackle Therapy Resistance in Melanoma. *Int. J. Mol. Sci.* **2022**, *23*, 3660. [[CrossRef](#)] [[PubMed](#)]
14. Wang, P.; Wang, Z.; Liu, J. Role of HDACs in normal and malignant hematopoiesis. *Mol. Cancer* **2020**, *19*, 5–26. [[CrossRef](#)] [[PubMed](#)]
15. Bondarev, A.D.; Attwood, M.M.; Jonsson, J.; Chubarev, V.N.; Tarasov, V.V.; Schiöth, H.B. Recent developments of HDAC inhibitors: Emerging indications and novel molecules. *Br. J. Clin. Pharmacol.* **2021**, *87*, 4577–4597. [[CrossRef](#)] [[PubMed](#)]
16. Pojani, E.; Barlocco, D. Romidepsin (FK228), A histone deacetylase Inhibitor and its analogues in cancer chemotherapy. *Curr. Med. Chem.* **2021**, *28*, 1290–1303. [[CrossRef](#)]
17. Zhang, L.; Zhang, J.; Jiang, Q.; Zhang, L.; Song, W. Zinc binding groups for histone deacetylase inhibitors. *J. Enzym. Inhib. Med. Chem.* **2018**, *33*, 714–721. [[CrossRef](#)]
18. Wang, Y.; Zhang, M.; Song, W.; Cai, Q.; Zhang, L.; Sun, X.; Zou, L.; Zhang, H.; Wang, L.; Xue, H. Chidamide plus prednisone, etoposide, and thalidomide for untreated angioimmunoblastic T-cell lymphoma in a Chinese population: A multicenter phase II trial. *Am. J. Hematol.* **2022**, *97*, 623–629. [[CrossRef](#)]
19. Hauschild, A.; Trefzer, U.; Garbe, C.; Kaehler, K.; Ugurel, S.; Kiecker, F.; Eigentler, T.; Krissel, H.; Schadendorf, D. A phase II multicenter study on the histone deacetylase (HDAC) inhibitor MS-275, comparing two dosage schedules in metastatic melanoma. *J. Clin. Oncol.* **2006**, *24*, 8044. [[CrossRef](#)]
20. Siliphaivanh, P.; Harrington, P.; Witter, D.J.; Otte, K.; Tempest, P.; Kattar, S.; Kral, A.M.; Fleming, J.C.; Deshmukh, S.V.; Harsch, A.; et al. Design of novel histone deacetylase inhibitors. *Bioorg. Med. Chem. Lett.* **2007**, *17*, 4619–4624. [[CrossRef](#)]
21. Hamoud, M.M.; Pulya, S.; Osman, N.A.; Bobde, Y.; Hassan, A.E.; Abdel-Fattah, H.A.; Ghosh, B.; Ghanim, A.M. Design, synthesis, and biological evaluation of novel nicotinamide derivatives as potential histone deacetylase-3 inhibitors. *N. J. Chem.* **2020**, *44*, 9671–9683. [[CrossRef](#)]
22. Hao, S.-Y.; Qi, Z.-Y.; Wang, S.; Wang, X.-R.; Chen, S.-W. Synthesis and bioevaluation of N-(3,4,5-trimethoxyphenyl)-1H-pyrazolo[3,4-b]pyridin-3-amines as tubulin polymerization inhibitors with anti-angiogenic effects. *Bioorganic Med. Chem.* **2020**, *31*, 115985. [[CrossRef](#)] [[PubMed](#)]
23. Sun, K.; Sun, Z.; Zhao, F.; Shan, G.; Meng, Q. Recent advances in research of colchicine binding site inhibitors and their interaction modes with tubulin. *Futur. Med. Chem.* **2021**, *13*, 839–858. [[CrossRef](#)] [[PubMed](#)]
24. Liu, W.; He, M.; Li, Y.; Peng, Z.; Wang, G. A review on synthetic chalcone derivatives as tubulin polymerisation inhibitors. *J. Enzym. Inhib. Med. Chem.* **2021**, *37*, 9–38. [[CrossRef](#)]
25. Ebenezer, O.; Shapi, M.; Tuszynski, J.A. A Review of the Recent Developments of Molecular Hybrids Targeting Tubulin Polymerization. *Int. J. Mol. Sci.* **2022**, *23*, 4001. [[CrossRef](#)] [[PubMed](#)]
26. Aboeldahab, A.M.A.; Beshr, E.A.M.; Shoman, M.E.; Rabea, S.M.; Aly, O.M. Spirohydantoins and 1,2,4-triazole-3-carboxamide derivatives as inhibitors of histone deacetylase: Design, synthesis, and biological evaluation. *Eur. J. Med. Chem.* **2018**, *146*, 79–92. [[CrossRef](#)] [[PubMed](#)]
27. Mourad, A.A.E.; Mourad, M.A.E.; Jones, P.G. Novel HDAC/Tubulin Dual Inhibitor: Design, Synthesis and Docking Studies of  $\alpha$ -Phthalimido-Chalcone Hybrids as Potential Anticancer Agents with Apoptosis-Inducing Activity. *Drug Des. Dev. Ther.* **2020**, *14*, 3111–3130. [[CrossRef](#)]
28. Bukhari, S.N.; Ejaz, H.; Elsherif, M.A.; Junaid, K.; Zaki, I.; Masoud, R.E. Design and Synthesis of Some New Furan-Based Derivatives and Evaluation of In Vitro Cytotoxic Activity. *Molecules* **2022**, *27*, 2606. [[CrossRef](#)]
29. Zaki, I.; Abu El-ata, S.A.; Fayad, E.; Abu Ali, O.A.; Abu Almaaty, A.H.; Saad, A.S. Evaluation of Synthetic 2,4-Disubstituted-benzo[g]quinoxaline Derivatives as Potential Anticancer Agents. *Pharmaceuticals* **2021**, *14*, 853. [[CrossRef](#)]

30. Zaki, I.; Abou-Elkhair, R.A.I.; Abu Almaaty, A.H.A.; Abu Ali, O.; Fayad, E.; Ahmed Gaafar, A.G.; Zakaria, M.Y. Design and Synthesis of Newly Synthesized Acrylamide Derivatives as Potential Chemotherapeutic Agents against MCF-7 Breast Cancer Cell Line Lodged on PEGylated Bilosomal Nano-Vesicles for Improving Cytotoxic Activity. *Pharmaceuticals* **2021**, *14*, 1021. [[CrossRef](#)]
31. Liu, Y.; Meng, Y.; Bian, J.; Liu, B.; Li, X.; Guan, Q.; Li, Z.; Zhang, W.; Wu, Y.; Zuo, D. 2-Methoxy-5((3,4,5-trimethoxyphenyl)seleninyl) phenol causes G2/M cell cycle arrest and apoptosis in NSCLC cells through mitochondrial apoptotic pathway and MDM2 inhibition. *J. Biochem. Mol. Toxicol.* **2022**, *3*, e23066. [[CrossRef](#)]
32. Nuth, M.; Benakanakere, M.R.; Ricciardi, R.P. Discovery of a potent cytotoxic agent that promotes G 2/M phase cell cycle arrest and apoptosis in a malignant human pharyngeal squamous carcinoma cell line. *Int. J. Oncol.* **2022**, *60*, 1–10. [[CrossRef](#)] [[PubMed](#)]